

Aeroelastic Investigation of Long Span Suspension Bridge Decks by Numerical CFD and FSI Analyses

Walid A. Latif Attia¹ Ahmed A. Aziz Ahmed²

1. Professor of Structure, Structural Engineering Department, Faculty of Engineering, Cairo University, Egypt

2. PhD Student, Assistant Lecturer, Structural Engineering Department, Higher Technological Institute, Egypt

Abstract

CFD (Computational Fluid Dynamics) simulations appear to be strong competitor of the wind tunnel test which required scaled model and it is really expensive and time consuming tool in designing bridges therefore there is a strong claim to replace them with CFD. Analyses carried out for different deck cross sections by secondary development of commercial computational fluid dynamics software ANSYS FLUENT, establishing two dimensional bending and torsional fluid-structure interaction (FSI) numerical model to calculate flutter critical wind speed. The flutter motion belongs to a sharp growth of amplitude (heave or rotation) as a function of the wind speed can be detected by performing the FSI at different wind speeds set in FLUENT model as a velocity inlet. By using the two neighboring wind speeds the critical wind speed can be obtained once a decay motion oscillation observed. Steady and unsteady simulations have been computed in order to judge the feasibility of CFD simulations in the early design stage of long span bridges. Additionally realizable (κ - ϵ) model with enhanced wall treatment and (κ - ω SST) turbulence models have been considered to verify their performance in bridge aerodynamics problems. It has been found that static aerodynamic coefficients have been correctly modeled using a steady simulation, while flutter critical wind speed is judged from time histories of unsteady simulations for stationary deck sections. The validity of the simulation method was verified by comparison of simulation results with the work done by other researchers.

Keywords: CFD, critical flutter wind speed, bridge aeroelasticity, suspension bridges.

1. Introduction

Wind load is one of the important design loads on civil engineering structures, especially for long span bridges with low damping and high flexibility. Deck sections of long span bridges are one type of bluff bodies that are usually elongated with sharp corners which make the flow around them to cause aerodynamic instabilities. Such instabilities may cause serious catastrophic structural failure such as, the Old Tacoma Narrows Bridge collapse in 1940. Suspension bridges not only must be designed to support the static wind forces like lift, drag and moment created by the mean wind, but also the dynamic loads created by an interaction between the wind forces and structural motions which known as aeroelasticity. Representative models are used in wind tunnel tests to obtain aerodynamic and aeroelastic information. However, with computers technology and CFD evolution, a lot of these problems can also be analyzed by numerical simulations.

Flutter occurs due to a structure and wind interaction where the wind speed has passed the critical speed of flutter and negative damping develops. If a structure is experiencing oscillation a positive damping will slowly decrease the amplitude of the displacement, on the other hand flutter increases the amplitude of the oscillation as time continues [8]. Figure 1 shows a sinusoidal representation of both positive and negative damping phenomena.

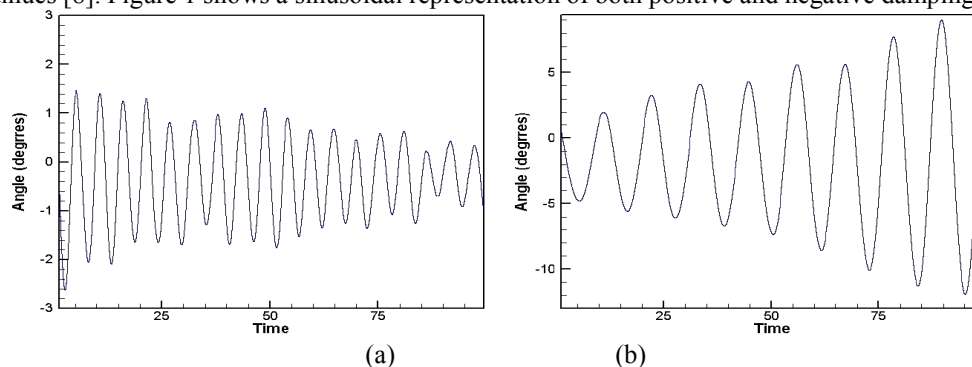


Figure 1: Example of (a) positive damping and (b) negative damping [5]

Galloping, vortex shedding vibrations, and flutter are the most aeroelastic phenomena that can be seen in long span suspension bridges. Only the last case will be studied in the present work and focused on producing a reliable results over a range of different bridge deck sections, establishing a dimensional bending and torsional fluid-structure interaction numerical model and finite element solver to calculate critical wind speed of flutter for different deck sections and determine whether a computational method can lead to a reduction in the number of expensive physical model tests.

2. Methodology

2.1 Numerical Simulation Principle

The structure is regarded as mass, spring and damping system. Schematic diagram of numerical simulation is shown in Figure 2. Fluid control equation for incompressible flow is the continuity and the Navier-Stokes equations (1) and (2). The first step to ascertain the aerodynamic response of the considered bridge deck types is computation of the force coefficients (C_d, C_l, C_m). After getting these coefficients, forces (F_D, F_L, M) can be easily calculated by equations. (3), (4), and (5). Figure 3 shows criteria for the aerodynamic forces and moment. The governing structural equations for heaving and torsional mode are equations (6) and (7).

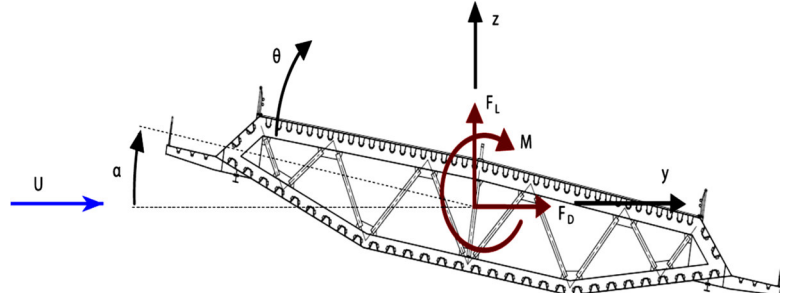
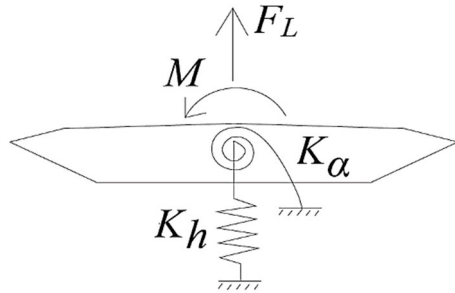


Figure 2: Schematic diagram of numerical simulation

Figure 3: Sign criteria for the aerodynamic Forces [3]

$$\nabla \cdot V^- = 0 \quad (1)$$

$$\frac{\partial V^-}{\partial t} + (V^- \cdot \nabla) V^- = -\frac{1}{\rho} \nabla p + \mu \nabla^2 V^- \quad (2)$$

$$F_D = 0.5 U^2 B C_d \quad (3)$$

$$F_L = 0.5 U^2 B C_l \quad (4)$$

$$M = 0.5 U^2 B^2 C_m \quad (5)$$

$$\dots \dots m \ddot{h}(t) + C_h \dot{h}(t) + K_h h(t) = F_L(t) \quad (6)$$

$$\dots \dots I \ddot{\alpha}(t) + C_\alpha \dot{\alpha}(t) + K_\alpha \alpha(t) = M(t) \quad (7)$$

Where:

V, p, t : Velocity, pressure, time respectively.

ρ : Air density.

μ : Air dynamic viscosity.

F_D, F_L, M : Drag force, lift force, and moment respectively.

C_d, C_l, C_m : Coefficients of drag force, lift force, and moment respectively.

U : Reference velocity.

B : Bridge width.

m : Deck mass per unit length.

I : Mass moment of inertia about shear center per unit length.

C_h, C_α : Structural damping coefficients.

K_h, K_α : Translational and rotational spring stiffness.

$\dots \dots \ddot{h}(t), \dot{h}(t), h(t)$: Instantaneous bending acceleration, velocity and displacement respectively.

$\dots \dots \ddot{\alpha}(t), \dot{\alpha}(t), \alpha(t)$: Instantaneous torsional acceleration, velocity and displacement respectively.

The critical velocity for bridges is calculated using FSI. The aeroelastic stability is observed from the free motion of the bridge deck for various wind speeds. The procedure of FSI simulation in every wind speed is shown in Figure 4.

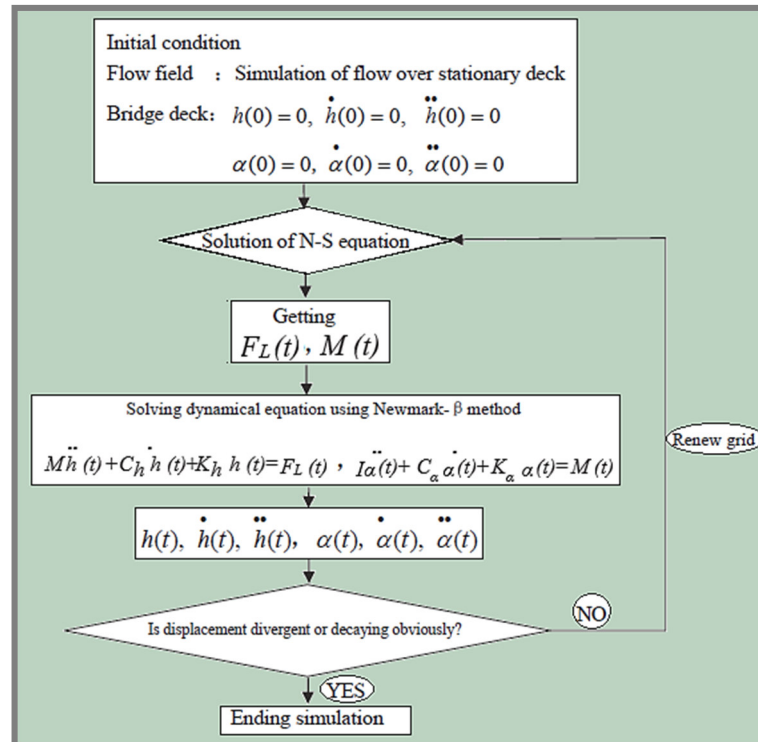


Figure 4: Procedure of FSI in every wind speed [8]

Static flow around bridge deck is performed and when the flow is stable, the bending torsional degrees are unrestricted. Before calculating time step, the preliminary value of bending and torsional acceleration, velocity, and displacement are set to be zero [6,9]. For every time step, the pressure and velocity are computed around bridge deck for the given position by solving the Navier-Stokes equations (1) and (2). Then calculate aerodynamic force coefficients acting on the bridge deck by using equations (4) and (5). This can be done by FLUENT [1, 8]. Lift pressure force and moment are represented by the force in y- direction and the force that causes rotation respectively. Lift force is applied at center of gravity and the moment is applied at the shear center. Then extract lift and moment into structural dynamic equations (6) and (7), then solve them by using Newmark- β method to get the displacements for heave and pitch. These displacements are applied in rigid body fashion and the grid is updated. The velocity of grid is applied from one time step to the next one by dividing time step size in difference position. This process is repeated for several time steps. Then the velocity of the grid is extracted in Navier stokes equations to account and simulate deck move by dynamic mesh technique. This can be done by secondary development of ANSYS FLUENT which program code is embedded to it by user defined function (UDF) [1]. Simulations of wind speed ends if the displacement divergent or decaying is observed. The critical velocity of flutter is found from plotting the time history of structure motion induced response.

2.2 Numerical Simulation Model

Four bridge deck sections were studied numerically using a commercially available CFD software in order to create an empirical reference set for numerical investigations. Among these section deck section (1) which belongs to the Great Belt East Bridge. Table 1 shows all full scale parameters of it. All deck sections have the same width equal to 31m and the same height equal to 4.4 m. Figure 5 shows the geometric definitions of them. CFD methodology for both steady and unsteady simulations is shown in Figure 6. 2D analyzed sections have been modeled by the incompressible turbulent of Navier-Stokes equations. There are two different equations of RANS (Reynolds Averaged Navier-Stokes) have been employed in the simulations: realizable (κ - ϵ) model with enhanced wall treatment and (κ - ω SST) Shear-Stress Transport. At inlet and outlet boundaries Dirichlet conditions have been committed; however at the deck sections surface no-slip conditions have been imposed. The turbulent flow characteristics has been defined with respect to intensity and viscosity ratio. For the pressure-velocity coupling implicit scheme for second-order and PISO algorithm are used. It is found that PISO scheme for pressure-velocity Coupling provides faster convergence for transient flow than the standard SIMPLE approach [1,2]. The time step was equal to 0.001 in Transient state simulations for (t^*) equal 60 seconds and the number of iteration per each time step equals 10. Unsteady simulations continued until a periodic behavior was reached. Computations have been carried out on core i7, 2.10 GHz, and physical memory 8.00 GB.

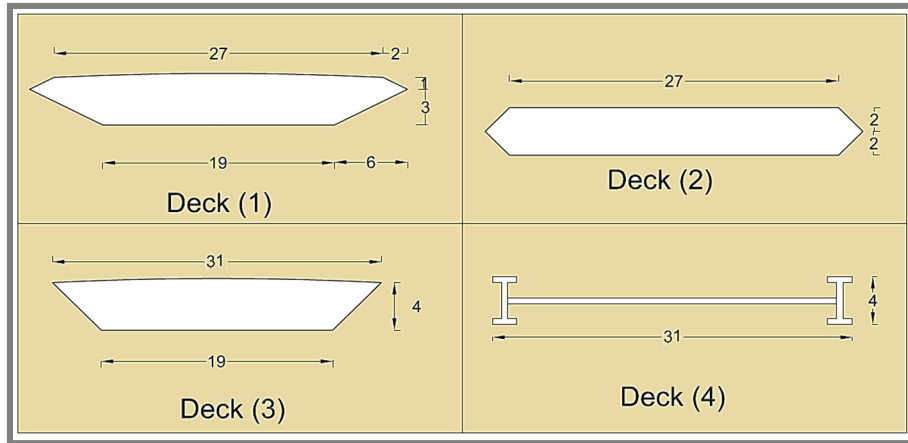


Figure 5: Geometric definition of the deck cross sections.

Table 1: Full scale properties of the deck section (1) (GBEB) [3]

Parameters	Units	Values
Natural vertical frequency (f_v)	Hz	0.097
Natural torsional frequency (f_t)	Hz	0.27
Mass per unit length (m)	kg/m	23 687
Mass moment of inertia about shear center per unit length (I)	Kg.m ² /m	2.501 x10 ⁶
Equivalent spring stiffness for vertical bending mode per unit length (K_b)	Kg/m ²	878.506
Equivalent spring stiffness for torsional mode per unit length (K_a)	Kg.m/m	7.194 x10 ⁵

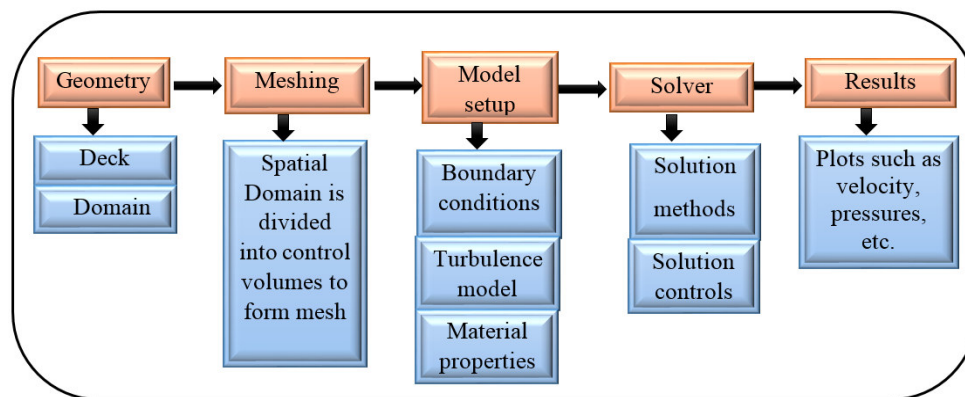


Figure 6: Flow chart for “CFD methodology” over bridge deck

2.2.1 Domain Simulation

The height of the fluid domain is 10 B and the length is 16 B where (B) is the width of the bridge deck. Rigid mesh grid is used in the inner region while stationary mesh grid is used in the outer region. Dynamic mesh grid is between the rigid mesh and stationary mesh. The width and height of rigid mesh are about two times and one time the width of the deck section respectively. Both the width and height of the dynamic mesh grid are about six times the width of the deck section. Figure 7 shows the domain regions and dimensions.

When deck section vibrates, the rigid mesh grid follows the deck section synchronously. The static grid keeps stationary while the shape and dimension of dynamic mesh changes constantly. In region which is far away from the deck section, the size of mesh grid is big comparatively on the contrary, the region which is near the deck section, the size of mesh grid is small comparatively.

Mesh information and size is defined by number of cells, nodes, and faces. Figure 8 and Table 2 show the definition of them. The whole numerical grids of the four sections of deck are shown in Figure 9.

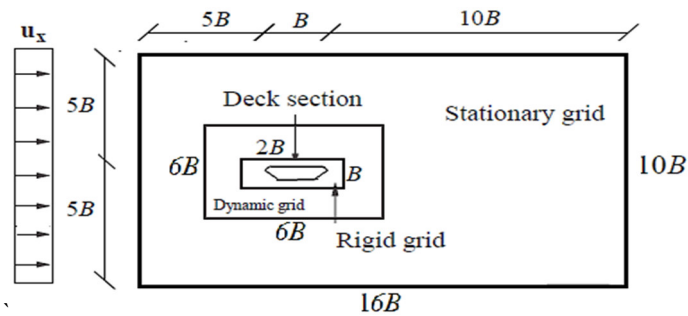


Figure 7: Domain regions and dimensions.

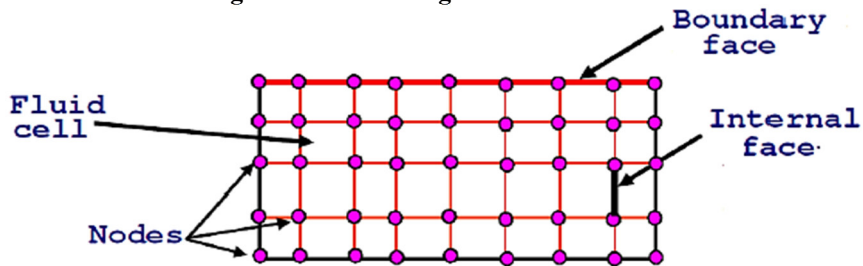


Figure 8: Definition of cells, nodes, and faces

Table 2: Mesh information for studied deck sections (CFD-Model)

Deck No.	Cells	Nodes	Faces
1	97360	53996	151356
2	95212	47969	143181
3	226424	113734	340158
4	155062	78274	233336

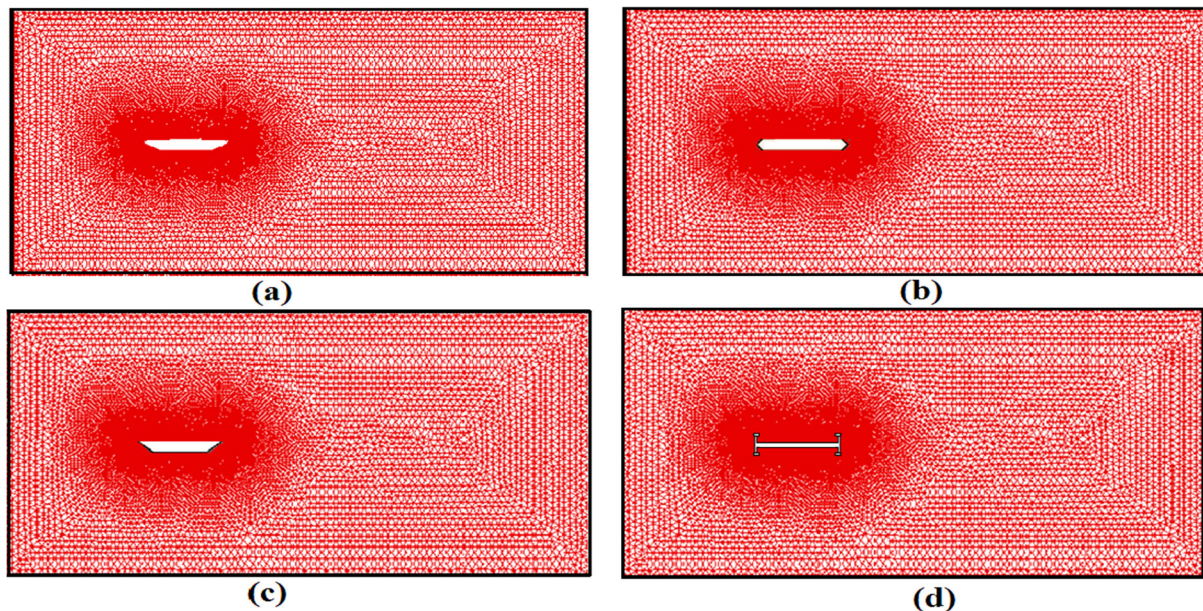


Figure 9: Whole mesh for different deck sections:

a) Deck section (1) b) Deck section (2) c) Deck section (3) d) Deck section (4)

2.2.2 Boundary Condition

The flow runs from the left to the right. The left side consider as inflow boundary specified with the velocity inlet. On the other right side an exit boundary specified with pressure outlet equal to zero. The upper and lower sides are specified as a symmetry. The deck edges are considered as a wall with no-slip boundary conditions.

3. Simulation Results

3.1 Steady Aerodynamic Force Coefficients

In order to validate the cross section geometry adopted for suspension bridges, the finite volume grid and the 2D

approach in the CFD analysis of the deck are used. Static aerodynamic coefficients have been computed assuming steady state for the deck. The aerodynamic coefficients have been computed for a Reynolds number equal 2.5×10^5 based on the deck width with different angle of attack in the range -10° to 10° with step 1° . Two different Reynolds-averaged turbulence models have been considered:

- 1- Realizable ($k-\epsilon$) with enhanced wall treatment.
- 2-Shear-Stress Transport ($k-\omega$ SST).

In each case of studied turbulence models second order scheme was used. The number of iterations was chosen 2000 in steady state simulations.

In Figure 10 the computed static aerodynamic force coefficients are presented along with the experimental results obtained by Félix Nieto [4] for the same Reynolds number and deck section (deck section 1). The computational results are very close to that which obtained from wind tunnel test. There are no significant differences in the results offered by ($k-\epsilon$) and ($k-\omega$) turbulence models. In general the static aerodynamic coefficients computed with ($k-\epsilon$) turbulence model are slightly lower than the ones computed using ($k-\omega$) turbulence model. From Figure 10 it can be concluded that mean force coefficients are in good agreement with the experimental data of the deck (1) section.

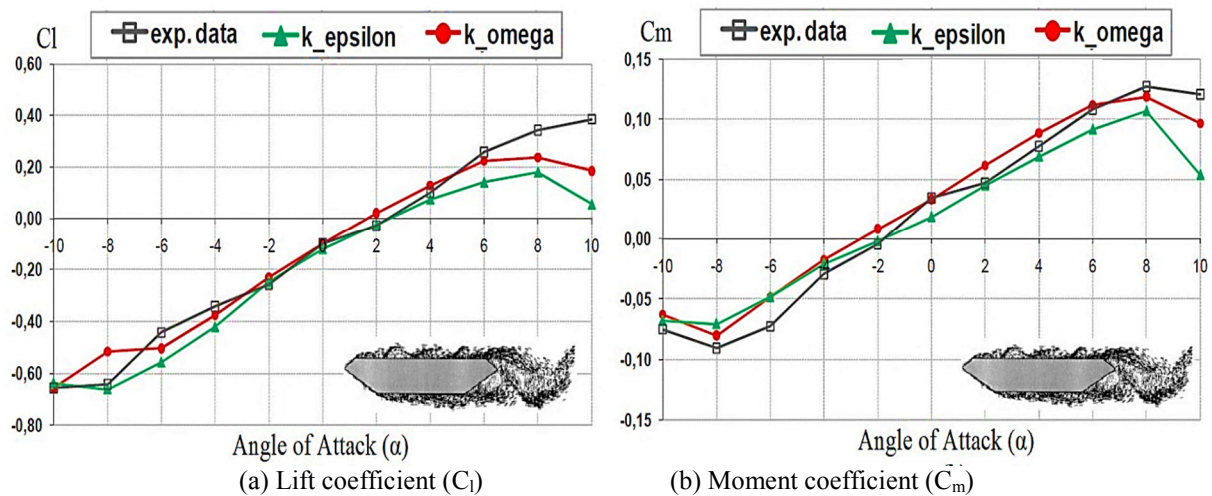


Figure 10: Aerodynamic coefficients of deck section (1) for ($Re=2.5 \times 10^5$).

3.2 Unsteady Time Histories Aerodynamic Coefficients

To find the critical wind speed of flutter for each deck cross section, Time history analysis for aerodynamic coefficients and vibrating motion should be applied by increasing the inlet velocity incrementally in different runs. When the aerodynamic coefficients and motion amplitude started growing (negative damping), the critical velocity was found. From Figures (11, and 12) for deck section (1) it can be seen that:

- (1) When wind speed is 68 m/sec, lift and moment coefficients are decreasing with the increase of time. This illustrates that the total damping of model is positive.
- (2) When wind speed is 69 m/sec, lift and moment coefficients remain almost same.
- (3) When wind speed reaches to 70 m/sec, lift and moment coefficients are increasing with the increase of time. This illustrates that the total damping of model changes from positive to negative. So Flutter critical wind speed is equal to 70 m/sec.
- (4) When flutter occurs, the torsional vibration frequency equal to 0.2 Hz. Comparing this frequency with those in Table 1 (f_v, f_i). This suggests that flutter style for deck section (1) is bending-torsional coupled flutter.

These previous investigations runs will now repeated for deck section 2, 3, and 4 until negative damping occur in each deck section. Table 3 and Figures (13, 14, and 15) show how critical wind speed of flutter is judged from time histories of unsteady simulations for different deck sections.

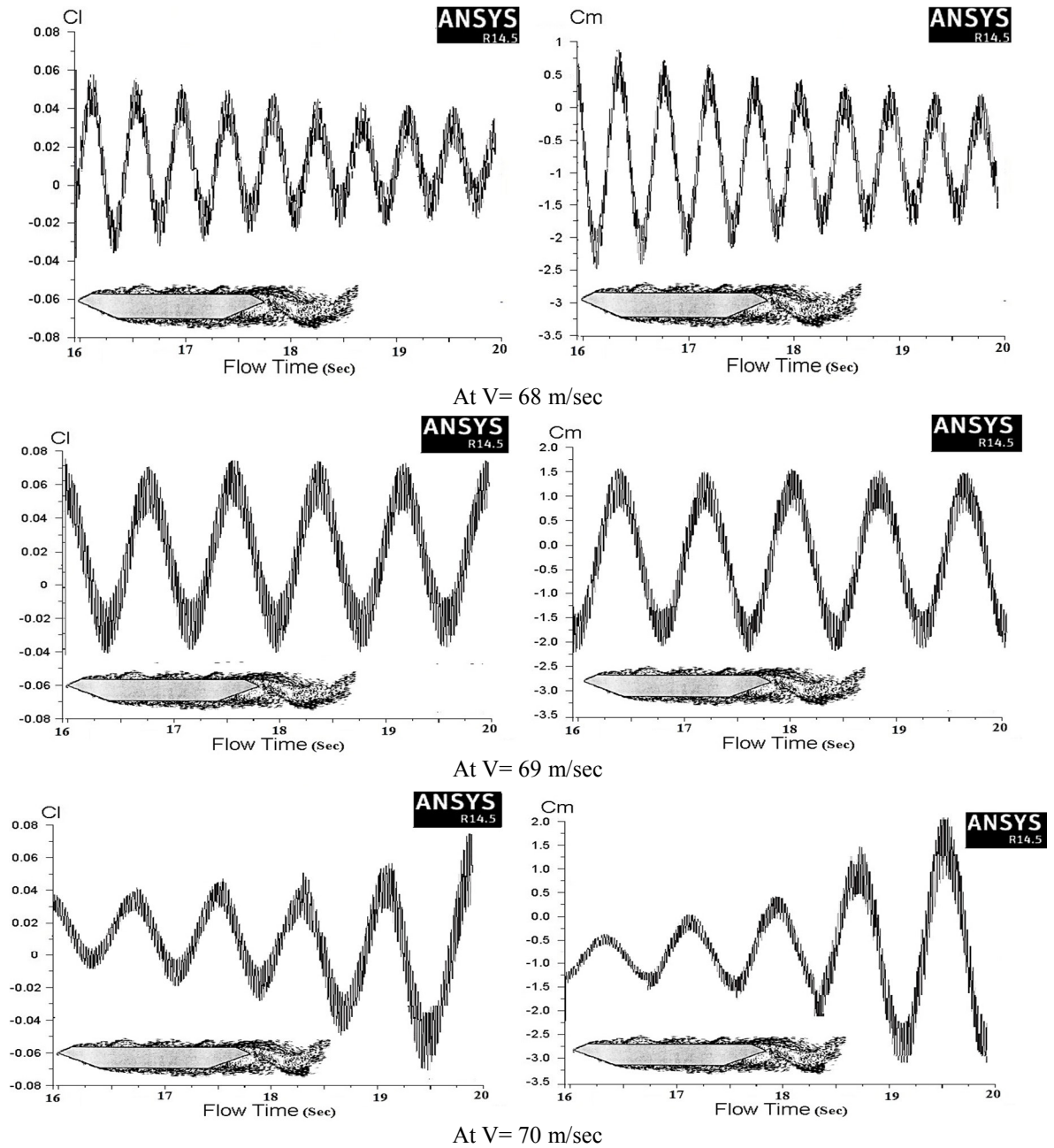


Figure 11: Time histories of lift and moment coefficients.

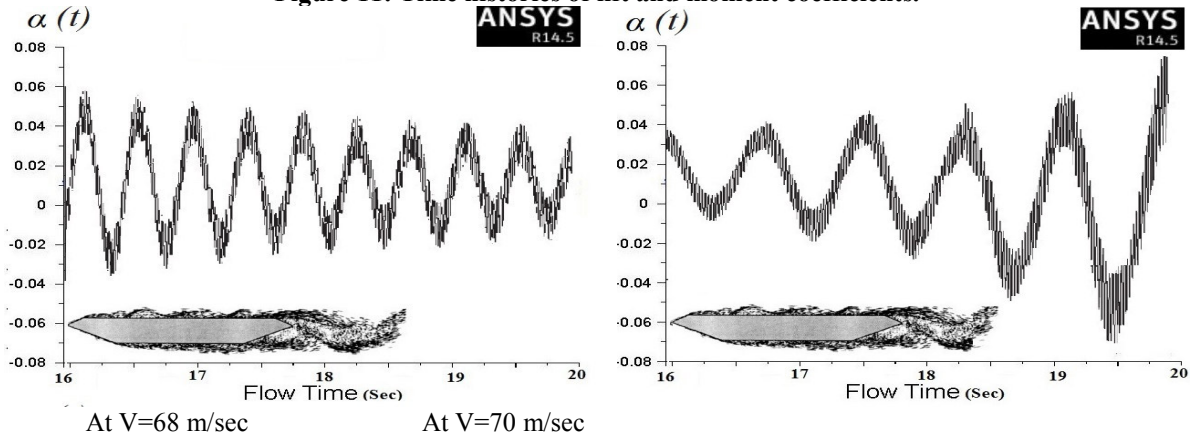


Figure 12: Time histories of torsional displacement for deck section (1)

Table 2: Getting flutter critical wind speed from time histories of unsteady simulations.

Deck cross section No.	1	2	3	4
The force acting on the deck gradually decreased at inlet velocity equal (positive damping)	68 m/sec	63 m/sec	60 m/sec	25 m/sec
The force acting on the deck gradually increased at inlet velocity equal (negative damping)	70 m/sec	64 m/sec	61 m/sec	26 m/sec
So Critical wind speed of flutter equal				
Figure No.	Figure 11 Figure 12	Figure 13	Figure 14	Figure 15

3.3 Comparison of Results

Steady simulations of the deck configuration considering a Reynolds number of 2.5×10^5 and range of angles of attack have offered aerodynamic coefficients close to the ones obtained from wind tunnel test for the same Reynolds number as shown in Figure 9. The results of the work done on deck section 1 is compared with other researchers as shown in Table 3. The critical flutter velocity predicted in present work is in good agreement with the wind tunnel results.

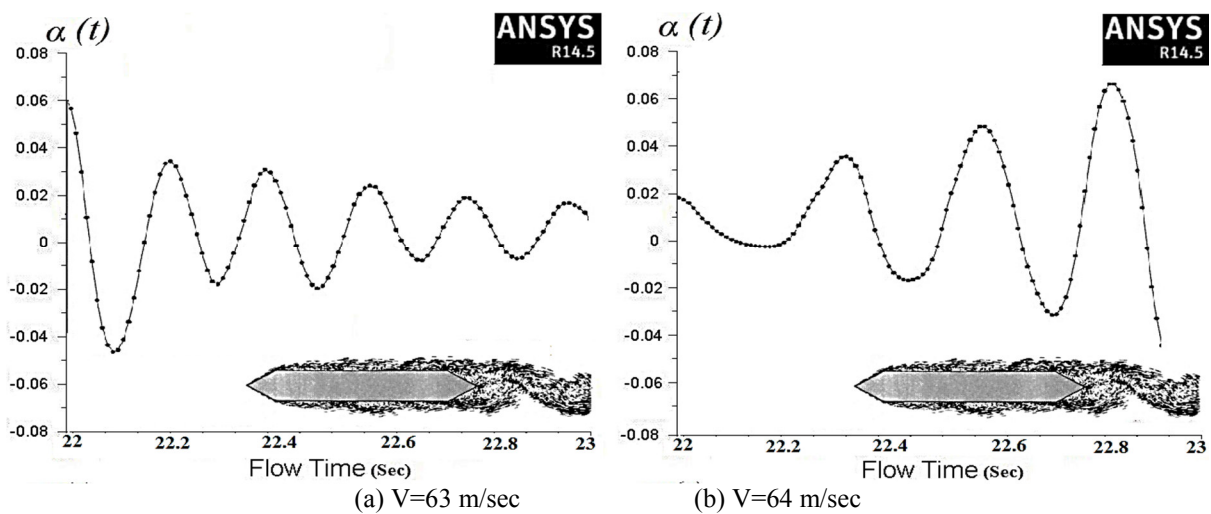


Figure 13: Time histories of torsional displacement for deck section (2).

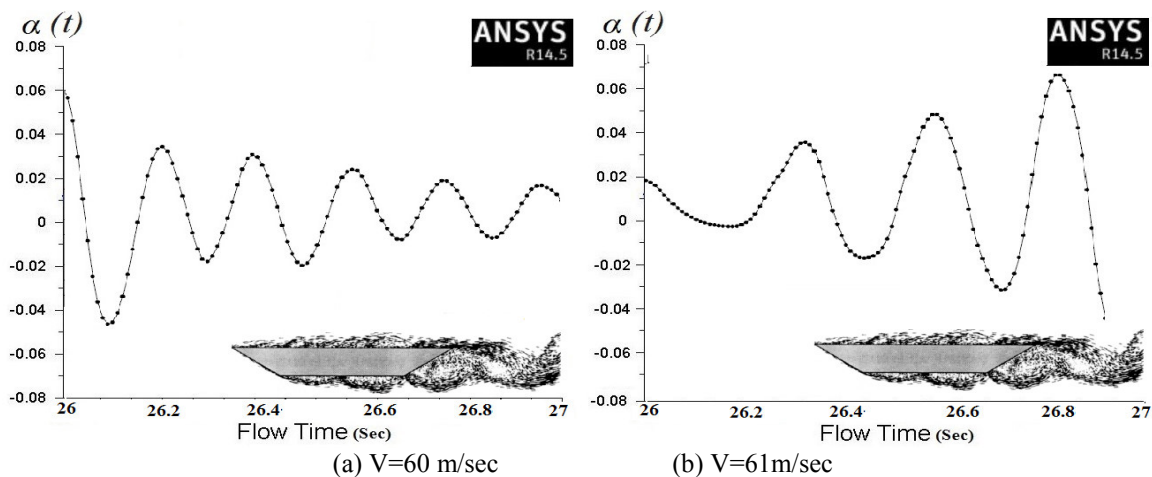


Figure 14: Time histories of torsional displacement for deck section (3).

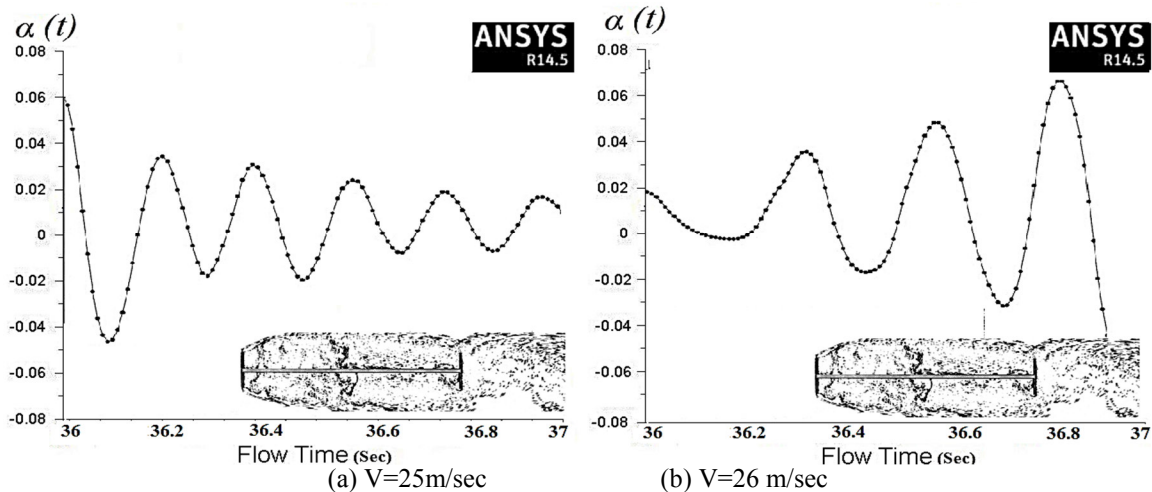


Figure 15: Time histories of torsional displacement for deck section (4).

Table 3: References of Flutter velocity for the Great Belt East Bridge.

Reference	Vcr (m/s)
Present work	70
Selvam et al. (2002)	65-72
Enevoldsen et. al.(1999)	70-80
Larsen et al. (1997)	74
Wind Tunnel Tests Larsen et al. (1998)	73

4. Conclusions

The following points offer the major outcome of the present study:

- 1- The shape of the deck of bridge is very important and as an outcome of the failure of the Tacoma narrow's Bridge, modern suspension bridges utilize trapezoidal box type sections or sharp leading edges sections like deck section (1 and 2) and solid girders must be avoided like deck section (4) .
- 2- The aerodynamics of bridge deck cross sections have been fully described through CFD simulations by the use of the software ANSYS. The viscous effects and the flow separation characterizing have been captured and included in the time history domain description of the aeroelastic loads.
- 3- Steady CFD simulation curves of the aerodynamic coefficients have been evaluated for a wide range of angles of attack and the computed results showed acceptable agreement between experimental and simulation for the same Reynolds number. Both turbulence models ($k-\epsilon$) and ($k-\omega$) performed similarly.
- 4- Unsteady 2D simulations of time history analysis for aerodynamic coefficients led to find the critical wind speed of flutter by increasing the inlet velocity incrementally in different runs. When the aerodynamic coefficient and motion amplitude started growing (negative damping), the critical wind speed was found.
- 5-The critical velocity for the onset of flutter was predicted successfully and is in good agreement with the wind tunnel results and work done by other researchers. The obtained critical flutter velocity for deck (1) is 70 m/sec agrees well with 73 m/s from the wind tunnel measurements.
- 6- FSI (direct simulation method) for flutter stability of bridge deck was developed based on CFD software FLUENT and proved to be useful in the early aerodynamic design stage of long span suspension bridges.
- 7- In the further FSI based on CFD will be used in studying of complex geometry deck of suspension bridges .

Acknowledgements

I am very grateful to Prof.Eman EL-Shamy, Structural Engineering Department, Zagazig University, Egypt and Dr. Szabó, Gergely, Structural Mechanics Department, Budapest University of Technology and Economics, Hungary for the many valuable comments to the manuscript.

References

- [1] Ansys Help, Release 14.5 Documentation for ANSYS, Fluid Dynamics, ANSYS FLUENT, Innovative turbulence modelling: in ANSYS FLUENT, (www.ansys.com).
- [2] Ashtiani Abdi, I. Experimental and Numerical Investigation of the Wind Effects on Long Span Bridge Decks. Master's thesis, Middle East Technical University, Turkey, (2011).
- [3] DMI and SINTEF, 1993b.Wind-tunnel tests.Storebalt East Bridge.Tender evaluation, suspension bridge. Alternative sections.Section model tests, I. Technical Report 91023-10.00. Revision .Danish Maritime Institute,

- Lyngby, Denmark.
- [4] Félix Nieto, Ibuki Kusano, Santiago Hernández, José Á. Jurado, CFD analysis of the vortex-shedding response of a twin-box deck cable-stayed bridge, The Fifth International Symposium on Computational Wind Engineering (CWE2010) Chapel Hill, North Carolina, USA May 23-27, 2010.
 - [5] Fok CH, Kwok KCS, Qin XR, Hitchcock PA. Sectional Pressure Tests of a Twin-deck Bridge: Part 2: Effects of Gap width on a Twin –deck Configuration. Proc. 11th Australasian Wind Engineering Society Workshop, Darwin, Australia; 2004.
 - [6] Gergely Szabó, József Györgyi and Gergely Kristóf, Advanced flutter simulation of flexible bridge decks, Coupled Systems Mechanics, Vol. 1, No. 2 (2012) 133-154.
 - [7] Hao Zhan, Tao Fang, Flutter stability studies of Great Belt East Bridge and Tacoma Narrows Bridge by CFD numerical simulation, The Seventh International Colloquium on Bluff Body Aerodynamics and Applications (BBAA7), Shanghai, China; September 2-6, 2012.
 - [8] Hao Zhan, Tao Fang, Zhiguo Zhang, Flutter stability studies of Great Belt East suspension bridge by two CFD numerical simulation methods, 6th European & African Conference on Wind Engineering, Robinson College, Cambridge, UK, July 7-11, 2013.
 - [9] Xiaobing Liu, Zhengqing, and Chenb Zhiwen Liu, Direct simulation method for flutter stability of bridge deck, The Seventh International Colloquium on Bluff Body Aerodynamics and Applications (BBAA7), Shanghai, China; September 2-6, 2012.